Journal of Applied Polymer Science

Transmission Electron Microscopic Observations of the Multilevel Microstructure of Crosslinked Copolymers with Methacrylates and Siloxane Macromers by a Radically Polymerizable Tuning Approach

Mitsuru Yokota,[1] Hiroharu Ajiro,[1,2] Mitsuru Akashi[1,2]

[1]Department of Applied Chemistry, Graduate School of Engineering, Osaka University, 2-1 Yamada-Oka, Suita, Osaka 565-0871, Japan

[2]The Center for Advanced Medical Engineering and Informatics, Osaka University, 2-2 Yamada-oka, Suita, Osaka, 565-0871, Japan

Correspondence to: M. Akashi (E-mail: akashi@chem.eng.osaka-u.ac.jp)

ABSTRACT: We investigated by Transmission Electron Microscopy (TEM) the morphologies of crosslinked copolymers from methacrylate monomers from methylmethacrylate (MMA) and trifluoroethylmethacrylate (TFEMA), polydimethylsiloxane (PDMS) macromers with molecular weight (Mn) of 1,700 and 4,700 g/mol, and crosslinker. Depending on the PDMS content, we observed, spherical PMMA islands in which small PDMS domains were dispersed, PMMA continuous phase, closely packed PTFEMA islands, and homogeneously dispersed PDMS domains were observed with low or middle magnification. Fine observation at 100,000-fold magnification revealed the "fundamental" common size domain, which was determined by the M_n value of the PDMS macromer. Thus we found two microstructure types: (1) a "fundamental domain" due to the M_n of the PDMS macromer, and (2) an aggregated domain. The former was constant under all conditions, but the latter was affected by the comonomer and its ratio. The present results are essential in understanding the chemical and physical characteristics of crosslinked copolymers from PDMS macromers. © 2012 Wiley Periodicals, Inc. J. Appl. Polym. Sci. 000: 000–000, 2012

KEYWORDS: siloxane macromer; morphology; transmission electron microscopy; fluoroalkyl group bearing vinyl monomer

Received 2 August 2011; accepted 22 March 2012; published online
DOI: 10.1002/app.37764

INTRODUCTION

Polymerization induced phase separation (PIPS)[1,2] is a convenient method to prepare microheterophases from a homogeneous solution of reactive monomeric compounds and polymeric compounds. This technique has been reported in many fields, such as the polymerizations of monomer/polymer mixtures,[3–5] preparation of hybrid porous polymer materials,[6,7] hydrogels,[8] or gel synthesis,[9] modified epoxy resins,[10,11] microencapsulation,[12] polymer-dispersed liquid crystals,[13,14] and so on.

On the other hand, many radically polymerizable silicone compounds have also been developed. The extremely high oxygen permeability of the silicone polymer contributed to the diverse applications of these products, and the problems inherent in silicone compounds, such as weak intermolecular force, the resultant fragility, and hydrophobicity have been improved. For example, the long Si—O—Si chain of polydimethylsiloxane (PDMS) was introduced into a polymer backbone via condensation reactions with a rigid segment, like polyamide and polyimide groups as multiblock copolymers.[15–18] Another approach is radical copolymerization among acrylic monomers with the macromer bearing a radically polymerizable group at the chain end of the PDMS, and the crosslinker which has multiple radically polymerizable groups.

PIPS technology using radically polymerizable PDMS macromers has been applied to copolymers with hydrophilic vinyl monomers[19–21] and hydrophobic vinyl monomers.[22,23] Studies on PIPS with hydrophilic vinyl monomers usually focus on the structure and dynamics of the resultant amphiphilic network, and PIPS examples of hydrophobic vinyl monomers show the effect of the monomer structures and the polymerizable groups of PDMS. It is one of the merits of radical copolymerization with vinyl monomers that the composition ratio and molecular weight (M_n) of PDMS macromer can be controlled. Thus, it is possible to perform a systematic study on the relationship between physical properties and copolymer compositions,

Table I. Molecular Weight of PDMS Macromer

Code	M_n from Manufacturer	M_n from NMR	Results from GPC		
			M_n	M_w	M_w/M_n
X	1720	1700	N.D.[a]	*	*
Y	4740	4500	4600	8300	1.80

[a]Not determined.

although there have been no reports on the PIPS microstructures generated from PDMS macromers, with systematic tuning of the composition and components, to our best knowledge.

As the part of aforementioned systematic study, we have already reported the high performance such as high oxygen permeability of PIPS method products from high M_n PDMS, compared with the material having low M_n silicone content.[24] In addition, it has been reported that the copolymerization of perfluoroalkyl ester group bearing monomer caused the increase of oxygen permeability.[25] Furthermore, we have found that larger M_n of PDMS and copolymerization of fluorine bearing monomer caused higher mobility than that from lower M_n PDMS or material without fluorine group.[26]

In this work, we focused on the internal microstructures observed by Transmission Electron Microscopy (TEM) for crosslinked copolymers composed of methacrylate monomers and PDMS macromers, and the relationship between the morphologies and their compositions was discussed. The TEM observation in this study could give some insight into the properties such as oxygen permeability and light transmittance.

EXPERIMENTAL

Materials

PDMS macromer was purchased from Shin-Etsu Chemical and was used without further purification. Molecular weight measurements by ^{1}H-NMR were conducted with a JEOL ECS400 spectrometer using $CDCl_3$ as the solvent, and GPC measurements were conducted by a HLC-8120 GPC system by TOSOH (Japan). The molecular weights of these PDMS macromers are listed in Table I. Methylmethacrylate (MMA) (Wako Pure Chemical Industries), trifluoroethylmethacrylate (TFEMA) (Osaka Organic Chemical Industry), ethyleneglycol dimethacrylate (1G) (Shin-Nakamura Chemical), 2,2′-azobis (2,4-dimethylvaleronitrile) (V-65) and 1,1′-azobis (cyclohexane-1-carbonitrile) (V-40) (both Wako) were used without further purification. The chemical structures of these monomers and the crosslinker are shown in Figure 1.

Preparation of the Crosslinked Copolymers Composed of Methacrylate Monomer/PDMS Macromer

The reaction mixtures were prepared by mixing the components according to the required balance, and degassing in a test tube. The mixtures were injected between a glass plate and a polytetrafluoroethylene film separated with a silicone elastomer gasket under a nitrogen atmosphere. The polymerization was then carried out by elevating the temperature from 50 to 110°C according to the predetermined temperature profile program.

As one of the methacrylate monomers, a fluoroalkyl group bearing TFEMA was used because of its low refractive index, comparable with that of silicone compounds, and some oxygen permeability. MMA was selected as another monomer because of its use as an optical material and its relatively high glass transition temperature (T_g).

The composition and other parameters of the test specimens are shown in Table II.

TEM Observation

The test specimens were cut from the crosslinked copolymer of 0.2 mm thickness, vacuum dried, and embedded in epoxy resin Quetol 812 (NISSHIN EM, Tokyo, Japan) without any staining. Ultrathin sections were cut with a diamond knife on an ultramicrotome, ULTRACUT E (Reichert-Jung Optishe Werke AG, Austria). The TEM observations were performed with a JEM 1200-EX transmission electron microscope (JEOL, Tokyo, Japan) at an accelerating voltage of 80 kV.

RESULTS AND DISCUSSION

Observations at Low Magnification

Without any staining of the specimens, all observations were carried out successfully as sufficient contrast was obtained for all specimens because of their electron density difference. Volume fraction was estimated with feed composition assuming that all constituents are not miscible, the density values were 0.98, 1.41, 1.19 for PDMS, PTFEMA, and PMMA including Poly(1G) respectively.

Figure 2 shows TEM images of all of the specimens listed in Table II at 20,000-fold magnification. Figure 2(a–c) are the results from specimens A, B, and C bearing 1700 g/mol M_n PDMS. According to the increase of PDMS content, which PDMS volume fraction is 0.2, 0.47, and 0.56 for specimen A, B, and C respectively, the domain size was decreased from 300 nm or more [Figure 2(a)], to 100–300 nm [Figure 2(b)], and to several 10 nm [Figure 2(c)], generating finer structures.

The PMMA enriched island possessing domain sizes of several μm was observed in specimens D (4700 g/mol of M_n) [Figure

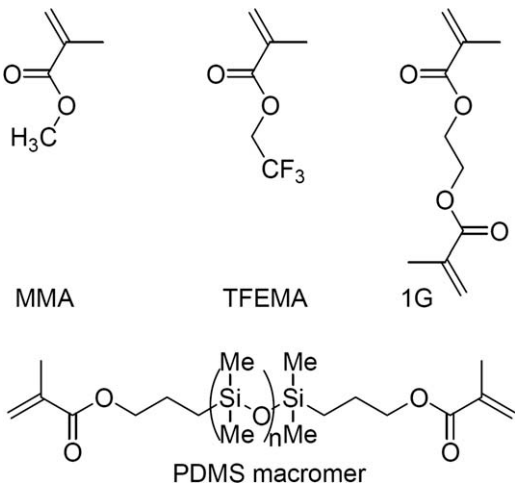

Figure 1. Chemical structures of the monomers and crosslinker.

Table II. Composition[a] of the Specimens Employed in This Study

	Acrylic monomer		PDMS macromer		PDMS[b]	
Code	Type	Weight	PDMS M_n	Weight	Weight fraction	Volume fraction
A	MMA	80	1700	20	0.17	0.20
B	MMA	50	1700	50	0.42	0.47
C	MMA	40	1700	60	0.51	0.56
D	MMA	70	4700	30	0.28	0.32
E	MMA	60	4700	40	0.38	0.42
F	MMA	40	4700	60	0.57	0.62
G	TFEMA	70	4700	30	0.28	0.36
H	TFEMA	60	4700	40	0.38	0.46
I	TFEMA	50	4700	50	0.47	0.56

[a]Parts of weight for 1G is acrylic monomer×(1/100) for all code, [b]PDMS weight fraction and volume fraction were calculated using PDMS weight which was obtained from the subtraction of the weight of methacryloyloxypropyl group from PDMS macromer. Volume fraction was estimated with feed composition assuming that all constituents are not miscible, the density value is 0.98, 1.41, 1.19 for PDMS, PTFEMA, and PMMA including Poly(1G) respectively.

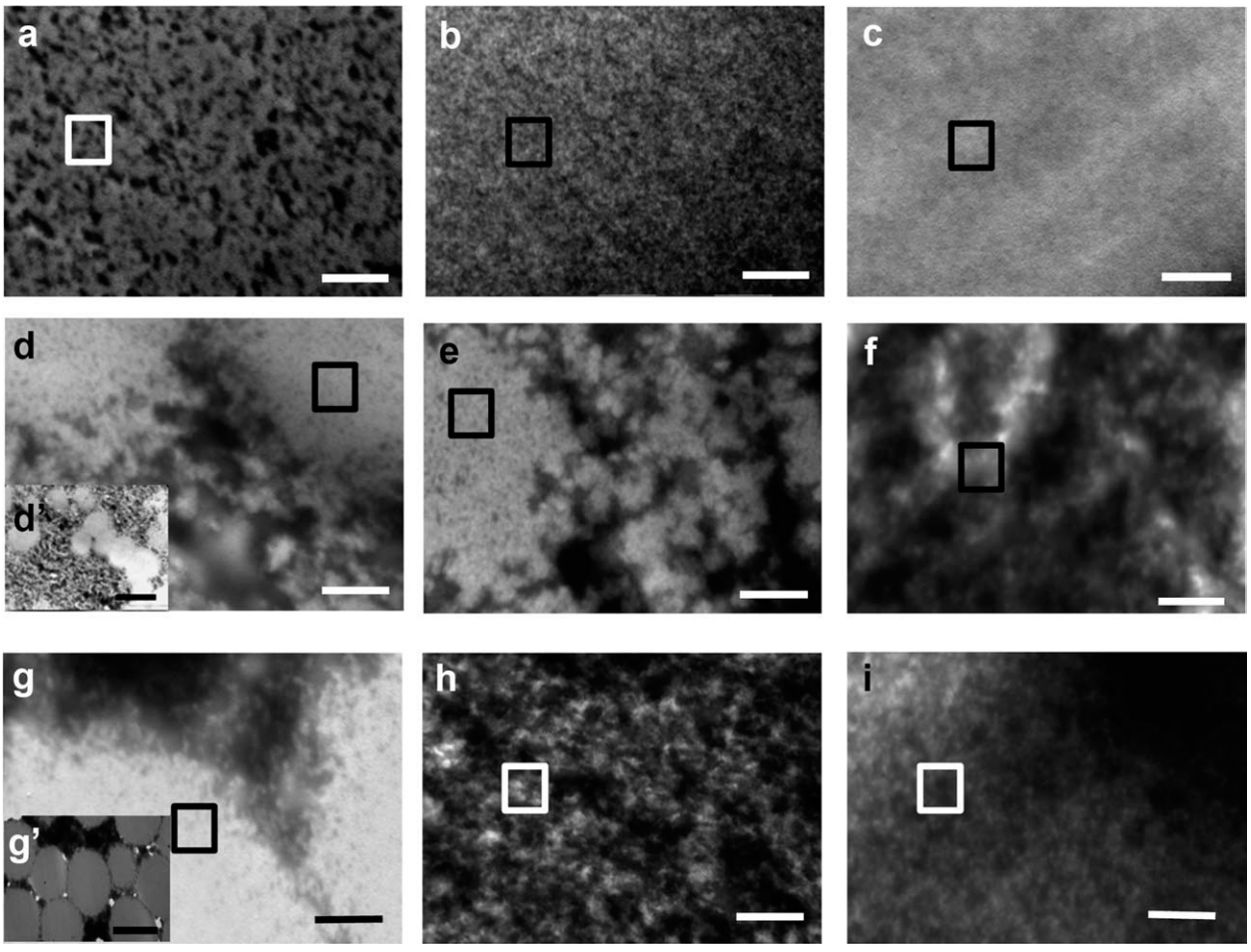

Figure 2. TEM images at 20,000-fold magnification of Specimen A (a), Specimen B (b), Specimen C (c), specimen D (d), specimen E (e), specimen F (f), specimen G (g), specimen H (h), and specimen I (i). Scale bar indicates 500 nm. Brighter and darker parts correspond to PMMA or PTFEMA rich phase and PDMS rich phase respectively. Inlet images d′ and g′ were obtained at 10,000-fold magnification. Scale bar in inlet indicates 5 μm. Square means observed position at 100,000-fold magnification in Figure 3.

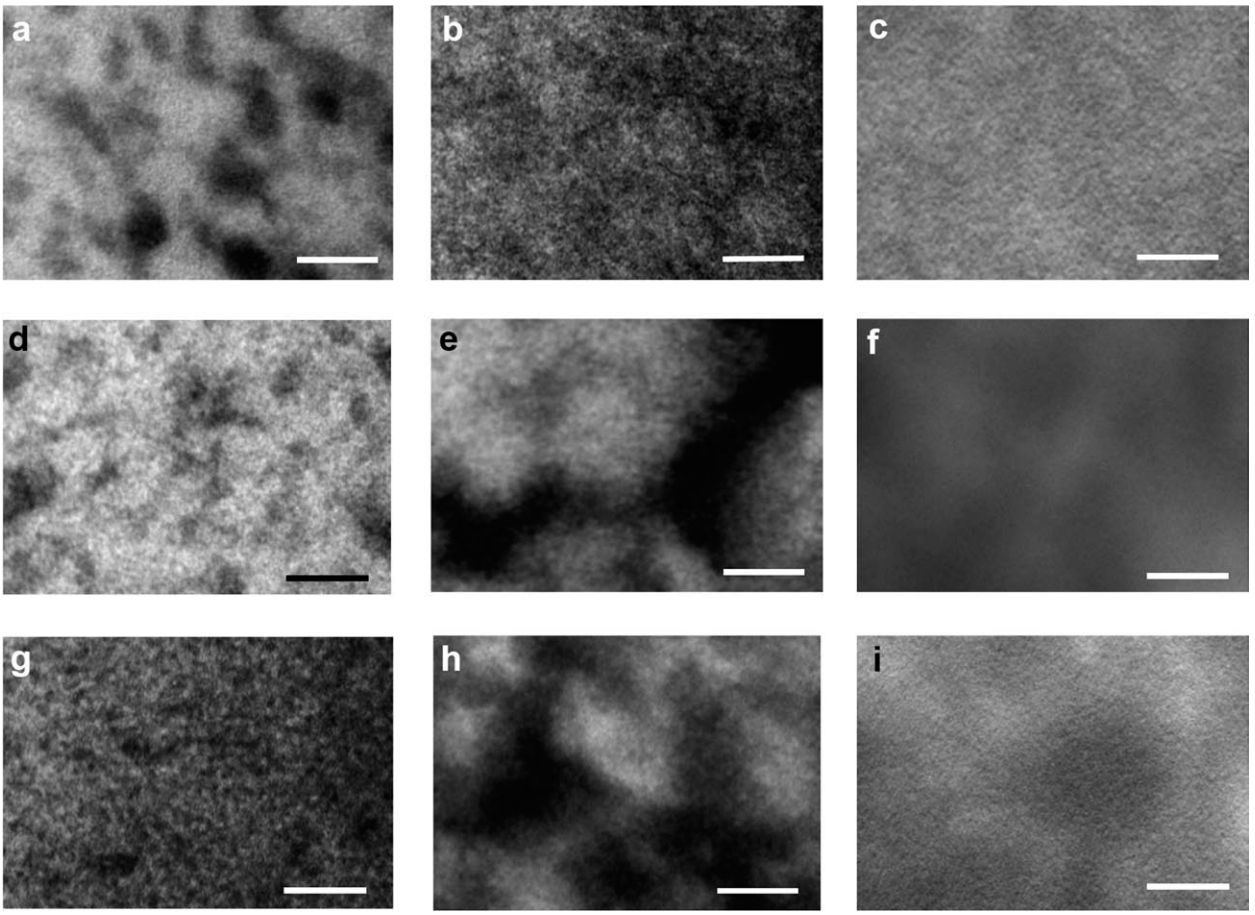

Figure 3. TEM images at 100,000-fold magnification of Specimen A (a), Specimen B (b), Specimen C (c), Specimen D (d), Specimen E (e), Specimen F (f), Specimen G (g), Specimen H (h), and Specimen I (i). Brighter and darker parts correspond to PMMA or PTFEMA rich phase and PDMS rich phase. Scale bar indicates 100 nm. Observed locations correspond to marked area in Figure 2.

2(d,d′)], which is quite different from specimen A [Figure 2(a)] with a similar volume fraction using the short PDMS chains. Comparing the results from specimen D with those from specimen E and F, with increase of PDMS content (PDMS volume fraction is 0.32, 0.42, and 0.62 for specimen D, E, and F, respectively), the domain size reduction of PDMS phase was found from several μm [Figure 2(d)] to 1–2 μm [Figure 2(e)] and sub-μm to μm size [Figure 2(f)].

With regards to specimen G [Figure 2(g)], in which TFEMA was copolymerized with PDMS (M_n = 4700 g/mol), the PTFEMA enriched island structure having several μm was also observed, which was clearly observed by inlet pictures with 10,000-fold magnification [Figure 2(g′)]. The contrast between the two phases was clearer than the aforementioned specimen D [Figure 2(d)], probably due to the composition of phases. The domain size in specimen G is larger than that of specimen D. Furthermore, most of the spaces between the islands seemed to consist of PDMS domains (dark parts), and the PDMS domains existed also in the PTFEMA islands at 20,000-fold magnification [Figure 2(g)]

In addition, with increase of PDMS content (PDMS volume fraction is 0.36, 0.46, and 0.56 for specimen G, H, and I, respectively), the domain size reduction of PDMS phase was also found from several μm (specimen G) to 500 nm (specimen H) and 200–300 nm size (specimen I) [Figure 2(g–i)].

TEM Observation at High Magnification

The TEM observation results at a high magnification (100,000-fold magnification) from all specimens are shown in Figure 3. Comparisons between Figures 2 and 3 with the same alphabetical letter suggested that, for example, the observation of specimens A at higher magnification (100,000-fold magnification) demonstrated that a microstructure appeared [Figure 3(a)] which was not observed in Figure 2(a). It is suggested that the new structure appearing *de novo* (dark part) was the coagulated small PDMS domain. Figure 2(b) (Specimen B) and Figure 2(c) (Specimen C) also showed fine structures and distributed PDMS domains, whereas Figure 3(b,c) showed the finer microstructure.

It is interesting that similar microstructures which have fine structure and coagulated PDMS domains of 100–200 nm size, were seen in Specimens D and G [Figure 3(d,g)], although difference in island/sea area ratio and that in dark/bright area ratio in the sea phase were seen between Figures 2d (or 2d′) and 2g (or 2g′). In addition, while difference in the domain size and pattern between Figure 2(e,h) was seen, Specimens E and H showed similar fine microstructure which consisted of fine

Table III. PDMS Measured Domain Size[a]

Code	Acrylic monomer	PDMS M_n	PDMS Volume fraction	Measured domain size (nm)
A	MMA	1700	0.20	4.3 ± 0.4
B	MMA	1700	0.47	4.3 ± 0.4
D	MMA	4700	0.32	5.5 ± 0.5
E	MMA	4700	0.42	5.1 ± 0.4
G	TFEMA	4700	0.36	5.4 ± 0.5
H	TFEMA	4700	0.46	4.8 ± 0.6

[a] $n = 30$.

structure and coagulated PDMS domains of 100–200 nm size at 100,000-fold magnifications [Figure 3(e,h)]. Similarly, while difference in the domain structure and domain size between Figure 2(f,i) was seen, Specimens F and I also showed similar fine microstructure which consisted of fine structure and coagulated PDMS domains of 100–200 nm size at 100,000-fold magnification [Figure 3(f,i)]. Thus, it is apparent that all of the observation results in Figure 3 at 100,000-fold magnification showed the minimum domain size or microstructure, which can be interpreted as them having almost the same "fundamental domain size."

To confirm this assumption, we measured the domain size on the TEM images using the loupe with 10 times greater magnification ($n = 30$). As shown in Table III, the domain sizes of the 1700 g/mol M_n PDMS were 4.3 nm (Specimen A) and 4.4 nm (Specimen B), whereas those of the 4700 g/mol M_n PDMS were 5.5 nm (Specimen D), 5.1 nm (Specimen E), 5.4 nm (Specimen G), and 4.8 nm (Specimen H), respectively. These values are appropriately correlated to the molecular weight of PDMS macromer when they were compared to the results of ca. 13.3 nm for the characteristic periodicity from the copolymer of polydimethylsiloxanediacrylate with 6500 g/mol M_n and the dimethylacrylamide reported by Yamamoto et al.[21] Therefore, it is suggested that the bulk properties are influenced by two types of microstructure at different magnification level; one of which is the microstructure consisting of the "fundamental domains" and the other is the microstructure consisting of the aggregation of "fundamental domains." For example, the oxygen permeability could be influenced not only by the "fundamental domain size," but also by the microstructure due to the aggregation of fundamental domains as suggested by Figure 3(d,g). On the other hand, the transparency could be influenced only by the microstructure from the aggregation of the fundamental domains.

This unique different type microstructure at different magnification level could be formed by the PIPS process as follow: In the first stage of PIPS process, due to the existence of large quantity of methacrylate monomer as solvent, fine structure (fundamental domain) in nm scale could be formed. While the progress in polymerization causes the reduction of methacrylate monomer as solvent, and this could lead to the phase separation or coagulation of fundamental domains in μm to sub-μm scales which are shown in Figure 2. The polymer properties such as miscibility and solubility parameter could affect the morphology of phase separation. Similar coexistence of μm scale structure and nm scale structure in spinodal decomposition of sol–gel process with various surfactant concentration.[27] Thus, it is suggested that PIPS is very important method to design and prepare the copolymer microstructure and resultant physical properties.

Correlation of the Morphology Between the Results from Low Maginification Level and High Magnification Level

For further understanding of this specific correlation of morphology, we conducted the TEM observation of islands phase and sea phase from Specimen D which showed highly phase separated internal structure from the copolymer of PDMS macromer ($M_n = 4700$ g/mol) with MMA at a 0.32 PDMS volume fraction. The observation results are shown in Figure 4.

It is noteworthy that many large (several μm) domains were observed in Figure 4(a) at 10,000-fold magnification. The PMMA enriched phase (bright part) existed as "islands" (isolated domains) at several μm order size, and the other composition phase in the spaces around the PMMA enriched islands showed the presence of both PDMS (dark part) and PMMA. At a higher 100,000-fold magnification [Figure 4(b)], in PMMA island, fine dark PDMS domains having several nm to 10 nm size and small amount of large PDMS domains (50–60 nm) were found in the bright continuous PMMA phase. On the contrary, in PDMS rich phase, fine dark PDMS domains having several nm to 10 nm size and large amount of more large PDMS domains having about 50–60 nm size were found. Thus, it was found that the present crosslinked copolymers possessed two types of phase separations with μm and nm orders in any composition, and the composition influenced the size of PDMS domain at the larger phase separation level. It was also demonstrated that the two phases possessed different PMMA/PDMS ratios, one of which was greater than 1.0 (the island part), and the other was near 1.0 (the sea part).

PDMS M_n, PDMS Content and Morphology at Low Magnification Level

As aforementioned, the PDMS M_n effect was clearly observed between the 1700 g/mol M_n and 4700 g/mol M_n PDMS. Lower M_n gave finer domain structure suggesting that the miscibility between PMMA or PTFEMA and PDMS affected the morphology.

It is natural that the transparency of the specimen appearance was related to its morphology. Specimens A, B, and C bearing 1700 g/mol M_n PDMS were transparent, and had small domain sizes of 300 nm or more [Figure 2(a)], 100–300 nm [Figure 2(b)], and several 10 nm [Figure 2(c)]. In contrast, Specimens D, E, and F with a 4700 g/mol M_n showed an opaque appearance due to light scattering at the domain boundaries of the several μm order size [Figure 2(d–f)]. Thus, it is important to understand the morphologies for the preparation of transparent samples, which is mostly due to the PDMS polymer chain length (PDMS M_n).

In addition, it was clear that a low PDMS content in the range of 0.2–0.36 volume fractions (Specimens D and G) caused the

Applied Polymer SCIENCE

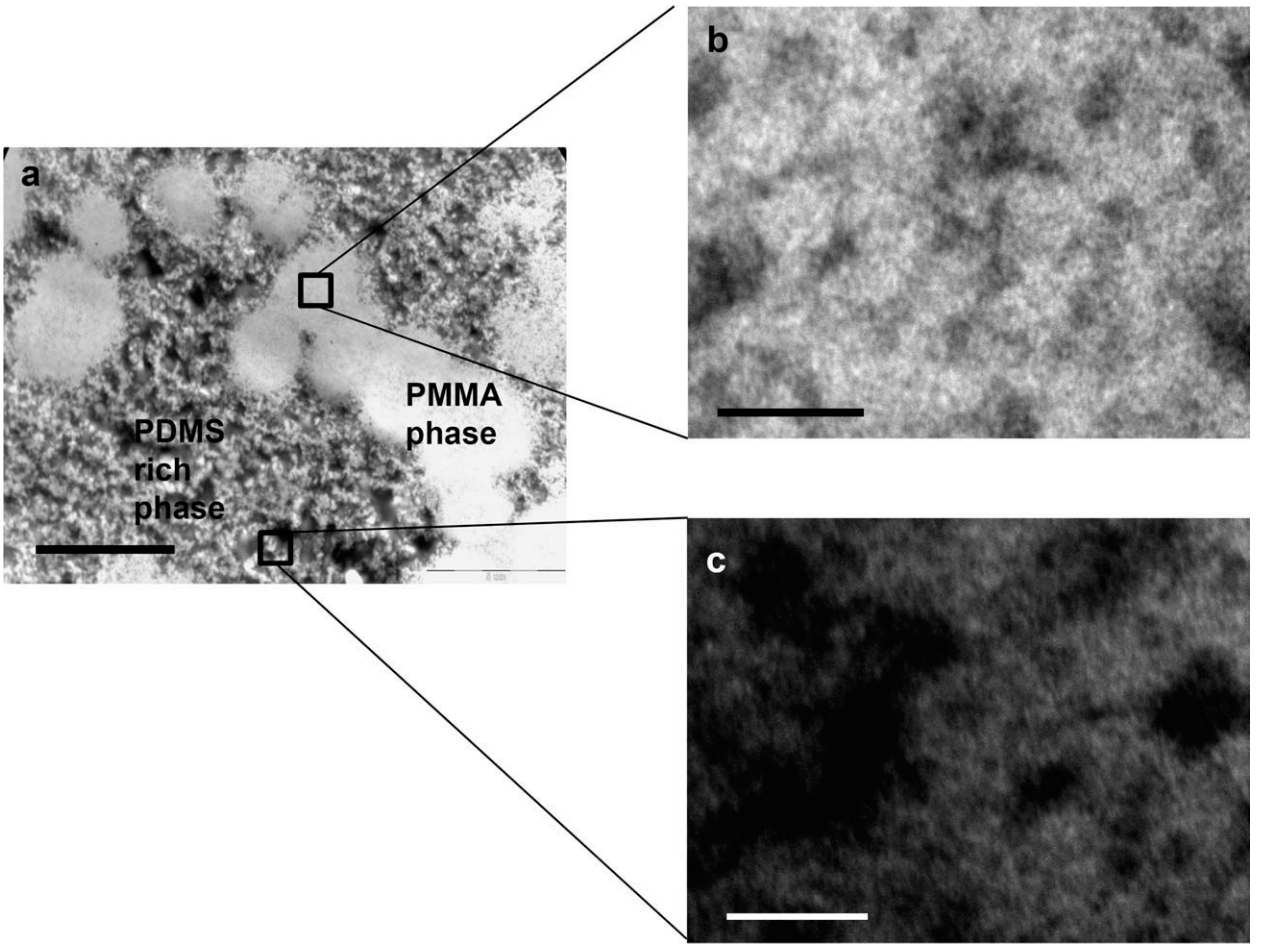

Figure 4. Correlation of the morphology between different magnification levels of Specimen D. (a) was obtained from 10,000-fold magnification. (b) and (c) are PMMA phase and PDMS rich phase respectively, and obtained from 100,000-fold magnification observation. Scale bar shows 5 μm (a), 100 nm (b, c). Bright phase is PMMA and dark phase is PDMS.

island shape of the methacrylate polymer phase [Figures 2d(2d′) and 2g(2g′)], although the island sizes were different. On the other hand, the middle PDMS content over the range of 0.56–0.62 volume fractions [Figure 2(c,f,i)] caused a domain size reduction, and a further continuous phase of the methacrylate polymer. Thus, by changing the composition or PDMS content systematically, the effect of the PDMS content on the morphology was clarified. The present results gave us essential information on the microstructure, because the morphology is closely associated with the bulk properties.

The importance of the polymerization mixture viscosity in the morphology formation of 2-chlorostyrene/polystyrene PIPS system has been reported by Okada et al.[5] It was reported that high viscosity caused the reduced polymer diffusion and this determined the degree of continuous phase formation. Thus island microstructure which was found in Specimens D and G [Figure 2(d,g)] could result from low viscosity with high monomer content (70 wt%), and the domain size reduction with increased PDMS content could result from high viscosity due to the PDMS M_n and two polymerizable groups in PDMS macromer in polymerization process.

Effects of the Methacrylate Monomer Type on Morphology

Next, the influence of the monomer types on the microhetero-phase structure was examined in detail using specimen D [Figure 5(a)] and Specimen G [Figure 5(b)]. We first noticed that Specimen D, which was copolymerized with MMA, left relatively small "island" shaped spheres that were rather scattered [Figure 5(a)]. In contrast, Specimen G with TFEMA resulted in larger ovals for the PTFEMA domains, and showed closely packed islands with small dark phases mostly composed of PDMS in the spaces between islands.

To consider the differences in the microphase separation by monomer type, we tried to estimate the area fraction of each "island" part from Figure 5(a,b) by calculating the percentages of the oval parts against the total area ($n = 3$). In spite of the same PDMS weight fractions (0.28), the values differed greatly, showing a 37% ratio for the PMMA islands in Specimen D and a 68% ratio for the PTFEMA islands in Specimen G. This implied that there were different components ratios in the other "sea" parts. In addition, PDMS phase (dark) of Figure 5(b) shows almost continuous one. Furthermore, comparison between Specimens F and I [Figure 2(f,i)] which have increased PDMS content than Specimens D and G, revealed that the

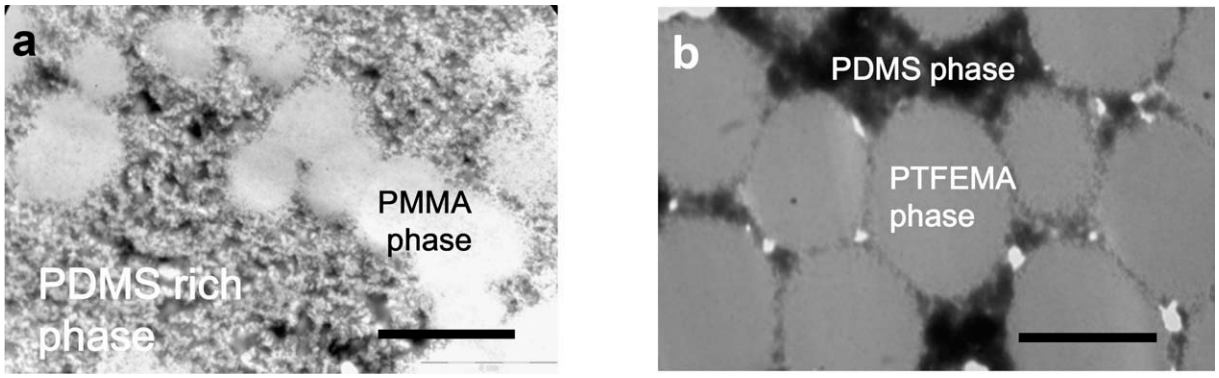

Figure 5. TEM images at 10,000-fold magnification for the comparison between Specimen D (a) and Specimen G (b). Scale bar indicates 5 μm. Small white area is due to the specimen defect from ultrathin sample preparation.

morphology of Specimen I correspond to the formation of the component's continuous phase. This formation of the continuous phase means a reduction in the barrier to oxygen permeation. Therefore, the copolymerization of PDMS macromer and TFEMA [Specimen I, Figure 2(i)] instead of MMA [Specimen F, Figure 2(f)] could lead to the formation of a morphology having more continuous phase. The oxygen permeability of the TFEMA copolymer would increase based on the phase separation difference, in addition to the original TFEMA character due to the fluoroalkyl groups. Thus, the higher oxygen permeability of the TFEMA copolymer than the MMA copolymer could be predicted from the TEM observations.[28]

CONCLUSIONS

TEM observation of crosslinked copolymers prepared from methacrylate monomers, PDMS macromers with M_ns of 1700 g/mol or 4700 g/mol, and 1G were carried out. The microstructure of these copolymers depended on the PDMS content, the PDMS M_n, and the type of methacrylate comonomer.

First, at low PDMS content, the specimens possessing 4700 g/mol PDMS M_n showed an "isolated domain" morphology with "islands" or isolated domains of methacrylate polymer dispersed throughout a "sea" like surrounding area. On the other hand, the specimens possessing 1700 g/mol PDMS M_n showed finer microstructures. At higher PDMS contents, a different morphology was observed, which consisted of a continuous phase of methacrylate polymer and more homogeneously dispersed PDMS domains.

Second, in addition to the PDMS M_n, the employment of TFEMA instead of MMA affected the morphology, such as a different island surrounding area phase composition or structure, and a more homogeneous structure suggestive of better solubility or compatibility between the TFEMA or PTFEMA and the other components.

Third, observations at 100,000-fold magnification revealed that the specimens had a "fundamental" common morphology, and it was a co-continuous one. From measurements of this domain size, the PDMS M_n was concluded to influence this PDMS "fundamental" domain size. Thus, studies using the observation of two microstructures could be a novel tool for evaluating the relationship between morphology and physical properties.

On the basis of those findings, many bulk properties could be predicted by morphology, such as T_g, transparency, and oxygen permeability.

ACKNOWLEDGMENTS

The authors are grateful to Professor Hirotaro Mori and Mr. Toshiaki Hasegawa at Research Center for Ultra-High Voltage Electron Microscopy, Osaka University for their arrangement and measurement with TEM.

REFERENCES

1. Yamanaka, K.; Inoue, T. *Polymer* **1989,** *30*, 662.
2. Inoue, T. *Prog. Polym. Sci.* **1995,** *20*, 119.
3. Wang, X.; Okada, M.; Han, C. C. *Macromolecules* **2007,** *40*, 4378.
4. Okada, M.; Inoue, G.; Ikegami, T.; Kimura, K.; Furukawa, H. *Polymer* **2004,** *45*, 4315.
5. Okada, M.; Fujimoto, K.; Nose, T. *Macromolecules* **1995,** *28*, 1795.
6. Dubinsky, S.; Petukhova, A.; Gourevich, I.; Kumacheva, E. *Macromol. Rapid Commun.* **2010,** *31*, 1635.
7. Ogasawara, S.; Kato, S. *J. Am. Chem. Soc.* **2010,** *132*, 4608.
8. Kwok, A. Y.; Prime, E. L.; Qiao, G. G.; Solomon, D. H. *Polymer* **2003,** *44*, 7335.
9. Nakanishi, K.; Amatani, T.; Yano, S.; Kodaira, T. *Chem. Mater.* **2008,** *20*, 1108.
10. Mueller, Y.; Haeussler, L.; Pionteck, J. *Macromol. Symp.* **2007,** *254*, 267.
11. Wang, M.; Yu, Y.; Wu, X.; Li, S. *Polymer* **2004,** *45*, 1253.
12. Kim, J.-W.; Lee, K.-S.; Ju, H.-K.; Ryu, J.-H.; Han, S.-H.; Chang, I.-S.; Kang, H.-K.; Oh, S.-G.; Suh, K.-D. *J. Polym. Sci. Part A: Polym. Chem.* **2004,** *42*, 2202.
13. Hoppe, C. E.; Galante, M. J.; Oyanguren, P. A.; Williams, R. J. *J. Macromolecules* **2002,** *35*, 6324.
14. Kyu, T.; Chiu, H.-W. *Polymer* **2001,** *42*, 9173.
15. Matsumoto, T.; Koinuma, Y.; Waki, K.; Kishida, A.; Furuzono, T.; Maruyama, I.; Akashi, M. *J. Appl. Polym. Sci.* **1996,** *59*, 1067.

16. Chen, S.-H.; Lee, M.-H.; Lai, J.-Y. *Eur. Polym. J.* **1996,** *32*, 1403.

17. Ha, S. Y.; Park, H. B.; Lee, Y. M. *Macromolecules,* **1999,** *32*, 2394.

18. Ghosh, A.; Sen, K. S.; Dasgupta, B.; Banerjee, S.; Voit, B. *J. Membr. Sci.* **2010,** *364*, 211.

19. Bruns, N.; Scherble, J.; Hartmann, L.; Thomann, R.; Iván, B.; Muellhaupt, R.; Tiller, J. C. *Macromolecules* **2005,** *38*, 2431.

20. Hanko, M.; Bruns, N.; Rentmeister, S.; Tiller, J. C.; Heinze, J. *Anal. Chem.* **2006,** *78*, 6376.

21. Yamamoto, K.; Ito, E.; Fukaya, S.; Takagi, H. *Macromolecules* **2009,** *42*, 9561.

22. Yu, X.; Nagarajan, M. R., Li, C.; Speckhard, T. A.; Cooper, S. L. *J. Appl. Polym. Sci.* **1985,** *30*, 2115.

23. Mazurek, M.; Kinning, D. J.; Kinoshita, T. *J. Appl. Polym. Sci.* **2001,** *80*, 159.

24. Yokota, M.; Goshima, T.; Itoh, S. *J. Brit. CL. Assoc.* **1992,** *15*, 125.

25. Koßmehl, G.; Fluthwedel, A.; Schäfer, H. *Makromol. Chem.* **1992,** *193*, 157.

26. Yokota, M.; Miwa, Y.; Ajiro, H.; Akashi, M. *Polym. J.* **2012,** *44*, 301.

27. Kanamori, K.; Kodera, Y.; Hayase, G.; Nakanishi, K.; Hanada, T. *J. Colloid Interface Sci.* **2011,** *357*, 336.

28. Yokota, M.; Ajiro, H.; Akashi, M. *J. Appl. Polym. Sci. in press.*